Cross-Sectional Dependence of Electron Mobility and Lattice Thermal Conductivity in Silicon Nanowires

E. B. Ramayya,[1] D. Vasileska,[2] S. M. Goodnick,[2] and I. Knezevic[1]

[1] *University of Wisconsin-Madison, Madison, WI 53706, USA*

[2] *Arizona State University, Tempe, AZ 85287, USA*

Email: ramayya@wisc.edu, knezevic@engr.wisc.edu

Abstract

The thermoelectric efficiency of a material depends on the ratio of its electrical and thermal conductivity. In this work, the cross-sectional dependence of electron mobility and lattice thermal conductivity in silicon nanowires has been investigated by solving the electron and phonon Boltzmann transport equations. The effects of confinement on acoustic phonon scattering (both electron-phonon and phonon-phonon) are accounted for in this study. With decreasing wire cross-section, the electron mobility shows a non-monotonic variation, whereas the lattice thermal conductivity exhibits a linear decrease. The former is a result of the decrease in intervalley and intersubband scattering due to a redistribution of electrons among the twofold-degenerate Δ_2 and fourfold-degenerate Δ_4 valley subbands when the cross-section is below 5×5 nm^2, while the latter is because of the monotonic increase of three phonon umklapp and boundary scattering with decreasing wire cross-section. Among the wires considered, those with a cross-section between 3×3 nm^2 and 4×4 nm^2 have the maximal ratio of the electron mobility to lattice thermal conductivity, and are expected to provide the maximal thermoelectric figure of merit.

Keywords: Acoustic phonon confinement, electron mobility, lattice thermal conductivity.

to appear in JCE, special issue: IWCE-12

I. INTRODUCTION

The thermoelectric (TE) figure of merit of a material is defined as $ZT = S^2\sigma T/(\kappa_l + \kappa_e)$, where S is the Seebeck coefficient, σ is the electrical conductivity, T is the absolute temperature, and κ_l and κ_e are the lattice and electronic components of thermal conductivity, respectively. ZT of a material has to be as high as possible for it to be used in TE applications. ZT of quasi-one-dimensional structures, such as nanowires, is much higher than that of their bulk counterparts primarily because of a reduction in phonon thermal conductivity κ_l due to enhanced phonon-boundary scattering and reduced acoustic phonon group velocity [1, 2]. While most previous work focused on Bi_2Te_3 as a potential candidate for solid-state TE applications due to its superior ZT, a recent study has shown that a SiGeC/Si superlattice microcooler can provide 6.9 K cooling at 100 °C heat sink temperature [3]. Silicon-based microcoolers would be ideal on-chip coolers due to the ease of integration with current microelectric devices.

Ultrathin silicon nanowires (SiNWs) are very attractive for TE applications, because they offer a relatively large reduction in thermal conductivity [4] compared to the reduction in the electron mobility μ [5]. Since $\kappa_l > \kappa_e$ and $\sigma \sim \mu$, a high TE efficiency can be obtained by maximizing μ/κ_l. In this study, we investigate the cross-section dependence of both μ and κ_l in square SiNWs to determine the SiNW cross-section that would be the most suitable for TE applications. The electron mobility was calculated using a Schrödinger-Poisson-Monte Carlo simulator developed previously [5, 6] and lattice thermal conductivity was calculated by solving the phonon Boltzmann transport equation under the relaxation time approximation, using Klemens-Callaway's expression modified to account for both boundary scattering and acoustic phonon confinement [2]. The confined acoustic phonon dispersion used in the acoustic phonon scattering rate calculations was obtained by using the *xyz* algorithm [7, 8].

The paper is organized as follows: in section 2, we emphasize the importance of considering acoustic phonon confinement in SiNWs by showing the discrepancy in the electron-acoustic phonon scattering rates calculated under bulk and confined mode approximations and by showing the reduction of acoustic phonon group velocity in SiNWs. In section 3, we present the variation of electron mobility and lattice thermal conductivity of SiNWs with cross-section. Concluding remarks are given in section 4.

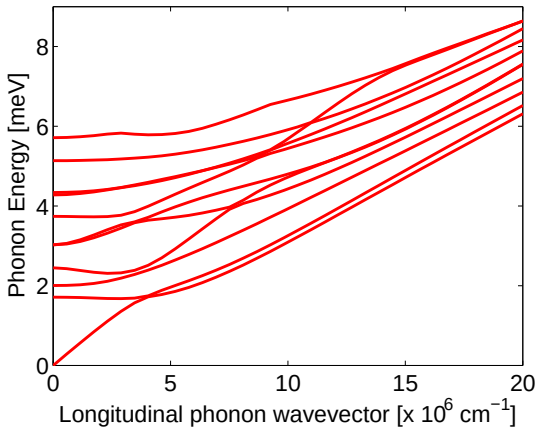

FIG. 1: Confined acoustic phonon dispersion calculated using the *xyz* algorithm [8] for an 8 × 8 nm^2 SiNW. Only the lowest 10 phonon subbands are shown.

II. CONFINED ACOUSTIC PHONONS

Acoustic phonons in SiNWs surrounded by SiO_2 are confined due to the difference in the dielectric and acoustic properties of Si and SiO_2. To get the confined acoustic phonon modes in SiNWs, we need to solve the elastic continuum equation subject to appropriate boundary conditions [9]. For a Si-SiO_2-Si sandwich structure, Donetti *et al.* have shown that the free-standing boundary condition (FSBC) gives reasonably accurate phonon modes [10]. Therfore, in this work, we have used the FSBC (normal component of stress tensor vanishes at each of the four Si-SiO_2 interfaces) to calculate the confined acoustic phonon modes. The acoustic phonon dispersion of the lowest 10 dilatational modes for an 8 × 8 nm^2 SiNW is shown in Fig. 1. Apart from the dilatational modes, there are two sets of flexural modes and one set of torsional modes in SiNWs. All four sets of modes are included in the calculation of both electron-acoustic phonon and acoustic phonon-acoustic phonon scattering rates. Fig. 2 shows the electron-acoustic phonon scattering rate for the lowest electron subband, calculated using both the bulk-mode and confined-mode approximations. When calculating the electron-bulk acoustic phonon scattering rates, acoustic phonon dispersion is assumed to be linear, $\omega_q = v_s q$, where v_s is the sound velocity. The resulting scattering rate, in the elastic and equipartition approximations [6], is proportional to the final electron density of states, and has the characteristic 1D density-of-states peaks (green dashed line) whenever the electron energy becomes sufficient to scatter into the next subband. In the case of confined

acoustic phonons, as seen in Fig. 1, the elastic approximation for electron-phonon scattering no longer holds, and neither does the linear dispersion at small wavevectors (except for the lowest phonon subband). Still, one can speak of a group velocity associated with a collection of phononic subbands. The average group velocity accounting for the non-uniform energy gap between different phonon modes is shown in Fig. 3. The average group velocity is close to the bulk value for very small phonon energies but it asymptotically reaches a constant value (less than 50% of its bulk value) at high phonon energies. Since the scattering rate due to confined phonon subbands is inversely proportional to their group velocity, on average, the confined acoustic phonon scattering rate is about two times the acoustic scattering rate calculated using bulk phonons (Fig. 2). Moreover, each of the bulk-phonon-scattering intersubband peaks in Fig. 2 (obtained in the elastic approximation, so the absorption and emission rate peaks coincide) splits into two groups of peaks (see Fig. 2) when confined phonons are considered: confined phonons can generally not be treated as elastic, hence there is a group of small peaks due to confined-phonon absorption below each bulk-phonon-scattering peak associated with a given electron subband, and a group of peaks due to confined-phonon emission above the bulk-phonon-scattering peak.

Acoustic phonons play a dominant role in both the electron-phonon scattering and in heat conduction, so it is important to include the effects of acoustic phonon confinement in the calculation of both the electron mobility and lattice thermal conductivity of SiNWs. In the rest of the paper, we will always assume confined acoustic phonons. Differences in the electronic and thermal properties of SiNWs that arise from using the bulk and confined acoustic phonon approximations will be addressed in detail in a forthcoming publication [5].

III. CROSS-SECTIONAL DEPENDENCE

The SiNWs considered in this study are similar to the channel of the ultra-narrow thin body SOI MOSFET that was originally proposed by Majima *et al.* [11]. The silicon channel is assumed to be homogeneous and infinitely long, and its cross-section is varied from 3×3 nm^2 to 8×8 nm^2.

Scattering of electrons due to confined acoustic phonons, Si-SiO_2 interface roughness and intervalley phonons are considered in the calculation of the electron mobility. The electron mobility variation with the wire cross-section for a very low transverse effective field from

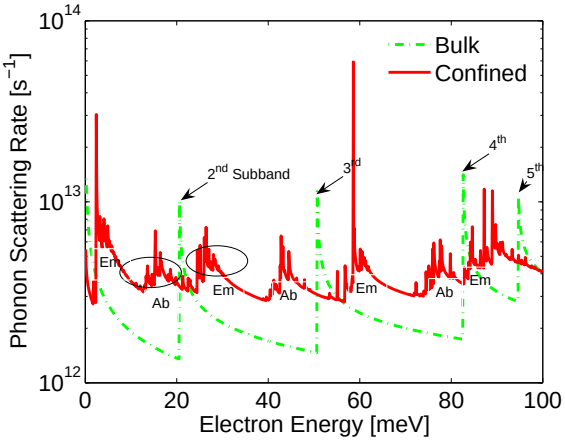

FIG. 2: Electron-acoustic phonon scattering rate for the lowest electron subband of an 8 × 8 nm^2 SiNW at the channel sheet density of $N_s = 8.1 \times 10^{11}$ cm^{-2}, calculated assuming the bulk and confined phonon approximations. The electron-bulk acoustic phonon intersubband spikes at around 20 meV, 52 meV, 85 meV, and 95 meV correspond to electron scattering from the lowest subband to the 2$^{\text{nd}}$, 3$^{\text{rd}}$, 4$^{\text{th}}$, and the 5$^{\text{th}}$ subband, respectively. To the left and right of each intersubband scattering spike corresponding to bulk phonon approximation are two groups of small spikes, corresponding to absorption ("Ab") and emission ("Em") of confined phonons from different phonon subbands.

the gate is shown in Fig. 4 (the transverse field from the gate is fixed at a very low value to resemble the ungated wire case relevant for thermoelectric applications). With increasing spatial confinement, the electron-phonon overlap integral [6] increases monotonically and results in a higher electron-phonon scattering rate. This is the reason for the mobility decrease observed when the wire cross-section decreases from 8 × 8 nm^2 to 5 × 5 nm^2. But, when the wire cross-section is further decreased, the decrease of intervalley and intersubband scattering due to the redistribution of electrons among the twofold degenerate Δ_2 and the fourfold degenerate Δ_4 valley subbands (Fig. 5) dominates over the increase in the electron-phonon scattering due to the increase in the overlap integral. Consequently, the mobility shows a shoulder at around 4.5 × 4.5 nm^2. Below this cross-section, virtually all electrons are in the lowest Δ_4-valley subband (4-fold degenerate), so the overlap integral again starts to dominate and the mobility rapidly falls [5]. It should be noted that the mobility variation for wires of cross-section larger than 7 × 7 nm^2 becomes very small. This is because of the interplay between a simultaneous increase in intersubband scattering (number of occupied

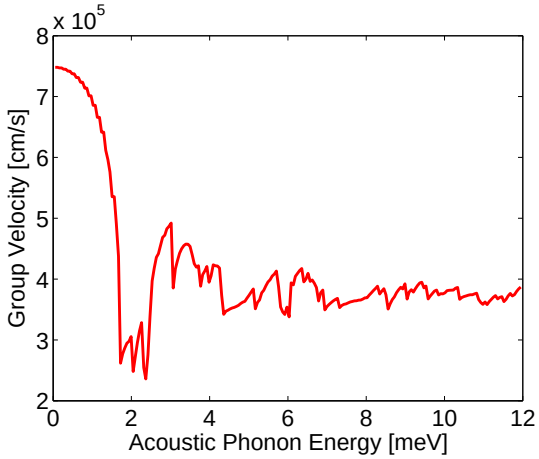

FIG. 3: Group velocity of dilatational modes for an 8×8 nm^2 SiNW. On average, acoustic phonon group velocity is reduced to less than 50% of the bulk value (9.13×10^5 cm/s).

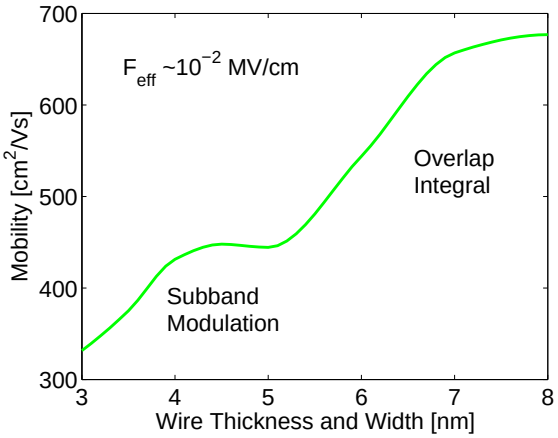

FIG. 4: Variation of the electron mobility with SiNW cross-section at a very low transverse field from the gate. Subband modulation (see Fig. 5) results in a reduction of intersubband and intervalley scattering.

subbands increases) and a decrease in intrasubband scattering (electron-phonon overlap integral decreases) with increasing wire cross-section. A similar weak dependence of the electron mobility in cylindrical SiNWs with diameters greater than 6 nm has also been reported by Jin *et al.* [12].

Lattice thermal conductivity is calculated by using a modified Klemens-Callaway expression derived from the phonon Boltzmann transport equation under the relaxation time approximation. The modified Klemens-Callaway expression accounts for both boundary

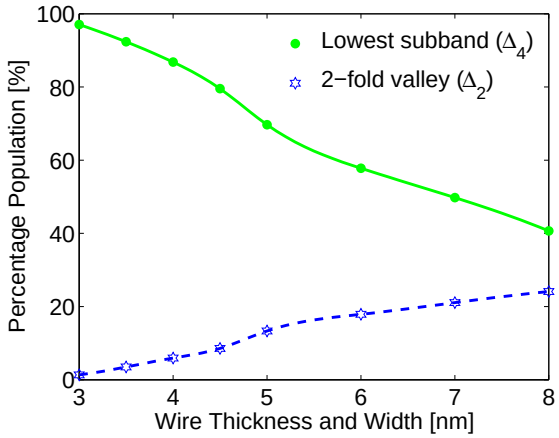

FIG. 5: Variation of the electron population among different valleys at a low transverse field (1.4 $\times 10^{-2}$ MV/cm). The solid line shows the total population of the electrons in the lowest subbands of Δ_4 valleys and the dashed line shows the population of the Δ_2 valley pair. Depopulation of electrons from higher Δ_4 subbands and the Δ_2 valley results in lower intersubband and intervalley scattering in ultranarrow SiNWs.

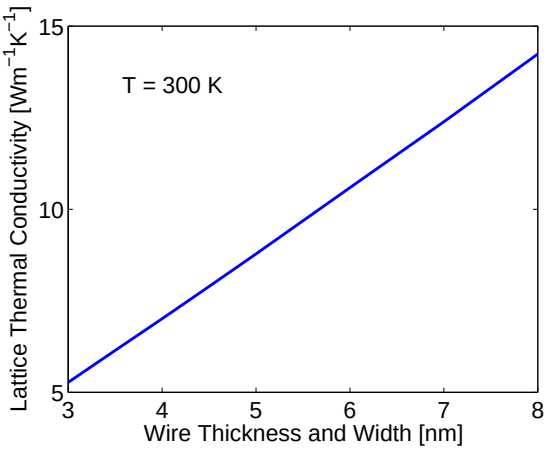

FIG. 6: Variation of the lattice thermal conductivity with SiNW cross-section, calculated at 300 K. Increase in boundary scattering and three-phonon scattering with decreasing wire dimensions results in a drastic reduction of κ_l in SiNWs.

scattering and acoustic phonon confinement [2]. The dominant scattering mechanisms, such as the three-phonon umklapp scattering and boundary scattering, are included in the calculation of the phonon relaxation rates. The effect of acoustic phonon confinement is accounted for by introducing the reduced acoustic phonon group velocity (Fig. 3) in the calculations.

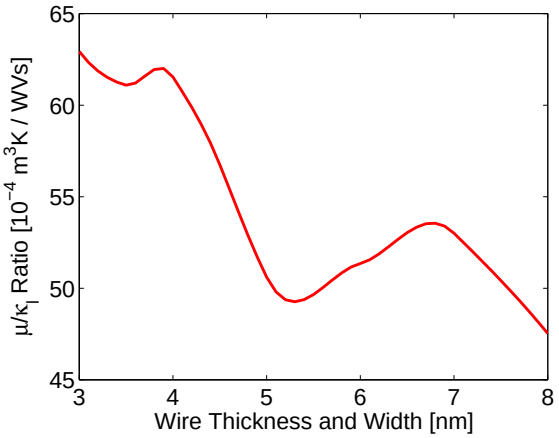

FIG. 7: Variation of the μ/κ_l ratio with the SiNW cross-section.

When calculating the acoustic phonon group velocity, we have accounted for the non-uniform energy gap between neighboring phononic bands, whereas previous studies [2, 13] have used only an average energy gap between phononic bands. This modification is very important, because the energy gap between different phononic bands strongly depends on the wavevector of the phonon. In this calculation, we have used the specular scattering fraction of 0.5 to describe the boundary scattering. Fig. 6 shows a linear decrease of the lattice thermal conductivity with decreasing SiNW cross-section. This decrease is due to the increase in both three-phonon umklapp and boundary scattering with the increase in spatial confinement of acoustic phonons. Thermal conductivity of SiNWs decreases by more than an order of magnitude from its bulk value of 148 $Wm^{-1}K^{-1}$.

Fig. 7 shows the variation of the μ/κ_l ratio with the SiNW cross-section. The μ/κ_l ratio exhibits a non-trivial variation with the wire cross-section due to the non-monotonic variation of μ with cross-section. Under the assumption that all the wires considered have the same carrier density, we would expect those with the largest μ/κ_l ratio to provide the maximum thermoelectric figure of merit. From Fig. 7 we can infer that, among the SiNWs considered, those with a cross-section between 3×3 nm^2 and 4×4 nm^2 have the highest μ/κ_l ratio.

IV. CONCLUSION

Electron mobility μ and lattice thermal conductivity κ_l have been calculated for SiNWs of different cross-sections, with the acoustic phonon confinement fully accounted for. Based on the variation of μ/κ_l with the wire cross-section, we expect the SiNWs with cross-sections between 3×3 nm^2 and 4×4 nm^2 to provide the maximum thermoelectric figure of merit. The effects of confinement on the electronic thermal conductivity κ_e and the Seebeck coefficient S were not considered in the present study, but they generally must be investigated to fully quantify the thermoelectric properties of SiNWs.

Acknowledgment

This work has been supported by the National Science Foundation through the UW MRSEC.

[1] L. D. Hicks and M. S. Dresselhaus, Phys. Rev. B **47**, 16631 (1993).

[2] X. Lü and J. Chu, J. Appl. Phys. **100**, 014305 (2006).

[3] X. Fan, G. Zeng, C. LaBounty, J. E. Bowers, E. Croke, C. C. Ahn, S. Huxtable, A. Majumdar, and A. Shakouri, Appl. Phys. Lett. **78**, 1580 (2001).

[4] D. Li, Y. Wu, P. Kim, L. Shi, P. Yang, and A. Majumdar, Appl. Phys. Lett. **83**, 2934 (2003).

[5] E. B. Ramayya, D. Vasileska, S. M. Goodnick, and I. Knezevic, *in preparation.*

[6] E. B. Ramayya, D. Vasileska, S. M. Goodnick, and I. Knezevic, IEEE Trans. Nanotechnol. **6**, 113 (2007).

[7] W. M. Visscher and A. Migliori and T. M. Bell and R. A. Reinert, J. Acoust. Soc. Am. **90**, 2154 (1991).

[8] N. Nishiguchi and Y. Ando and M. N. Wybourne, J. Phys. Condens. Matter **9**, 5751 (1997).

[9] E. P. Pokatilov, D. L. Nika, and A. A. Balandin, Phys. Rev. B **72**, 113311 (2005).

[10] L. Donetti and F. Gámiz and J. B. Roldán and A. Godoy, J. Appl. Phys. **100**, 013701 (2006).

[11] H. Majima and H. Ishikuro and T. Hiramoto, IEEE Electron Device Lett. **21**, 396 (2000).

[12] S. Jin, M. V. Fischetti, and T.-W. Tang, J. Appl. Phys. **102**, 083715 (2007).

[13] J. Zou and A. Balandin, J. Appl. Phys. **89**, 2932 (2001).